Halbach 배열 영구자석형 Planar Motor의 수직력 최소화

論 文
55B-11-7

Normal Force Minimization of the Synchronous Permanent Magnet Planar Motor with Halbach Magnet Array

金 德 顯* · 金 奎 卓†
(Duk-Hyun Kim and Gyu-Tak Kim)

Abstract - This paper presents the characteristics analysis and normal force minimization of a synchronous permanent magnet planar motor(SPMPM) with Halbach magnet array. Firstly, the flux density distribution is calculated by analytical method; then, the characteristics of this SPMPM are evaluated, some experiments have been done to verify the analysis propriety and to investigate the interaction among the characteristics; At last, the normal force is minimized by using genetic algorithm and it is decreased from 672.83[N] to 144.24[N] remarkably.

Key Words : SPMPM, Halbach magnet array, Genetic algorithm, Minimization of normal force,

1. INTRODUCTION

Planar motors are widely applied in many industry fields such as components insertion system, integrated-circuits fabrication, precision metal-cutting, etc. Compared with the conventional system using two linear motors to achieve a surface motion, the planar motor has the advantages such as direct driving and high accuracy. Especially, the synchronous permanent magnet planar motor(SPMPM) is widely used because of its low cost, simple structure, high energy density, etc [1] - [3].

This study focuses on the thrust, normal force and its minimization of the SPMPM. The flux density of Halbach magnet arrays, back-EMF and thrust have been analyzed by means of analytical method [4]. To verify the propriety of characteristics analysis, simulation values are compared with experimental values. Simulation values of magnet flux density and back-EMF accord with experimental ones well. But, experiment values of the thrust are smaller than the simulation ones because of the friction force which is generated greatly by normal force. So, it is necessary to minimize the normal force of SPMPM.

In this paper, the normal force minimization of SPMPM is presented and it is achieved by using genetic algorithm. The characteristics of original model and optimal model are compared.

† 교신저자, 正 會 員 : 昌原大學校 工大 電氣工學科 敎授
E-mail : gtkim@sarim.changwon.ac.kr
* 正 會 員 : 建東大學校 機電工學部 助敎授 · 工博
接受日字 : 2006年 9月 29日
最終完了 : 2006年 10月 13日

2. MODEL AND MAGNET FIELD ANALYSIS

A. Analysis model and dimensions

Fig. 1 shows a prototype machine of the SPMPM with Halbach magnet array. It has the mover with four sets of three-phase armature windings and the stator on which the Halbach magnet arrays are mounted . Two sets of armature windings are used to drive the mover in x direction and the others are used to drive the mover in y direction. The dimensions of this SPMPM are described in Table 1. The parameters interpretation of Halbach magnet array can be seen in paper[4]. Fig. 2 shows the shape of armature windings.

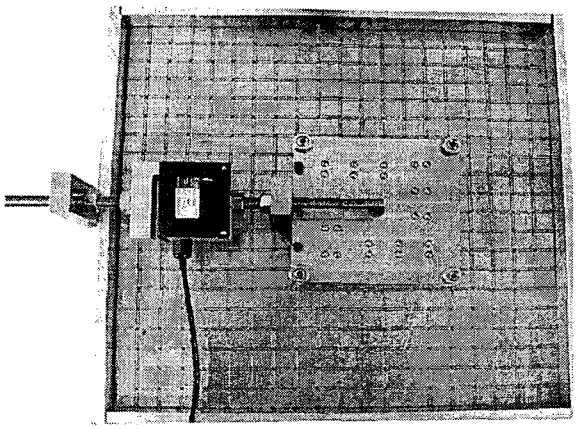

Fig. 1 The Prototype machine of the SPMPM

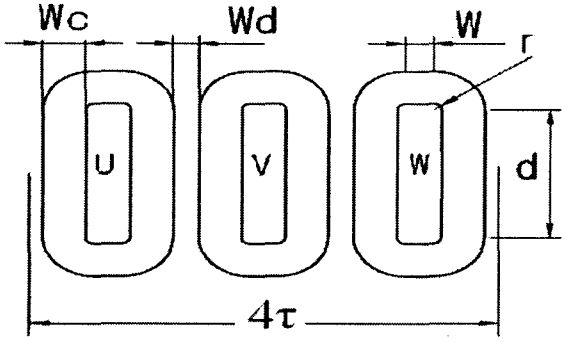

Fig. 2 The shape of armature winding

Table 1 Dimensions of the prototype machine

Part	Item	Symbol	Quantity	Unit
Permanent Magnet	Relative permeability	μ_r	1.05	
	Residual flux density	B_r	1.3	T
	Pitch	τ	20	mm
	Thickness	l_m	10	mm
	Width	p	18	mm
Mechanical air-gap	length	l_s	1	mm
Armature winding	Width	w_c	9	mm
	Terminal length	w	6.6	mm
	Effective length	d	20	mm
	Inner radius	r	0.5	mm
	Phase interval	w_d	1.03	mm
	Thickness	l_c	6	mm
Turns/phase		N_t	770	

B. Magnet field in the air-gap of SPMPM

The magnet flux density is obtained by using magnetic scalar potential and the process of analysing the magnet flux density generated by the permanent magnet arrays is presented in paper [4], the magnet flux density produced by the current in armature windings is deduced by the same method. The magnet flux density in the air gap can be fellowing

$$B_x = \sum_{k=1,3...}^{\infty}\sum_{l=1,3...}^{\infty}\left[\begin{array}{l}K_{xy}^{pm}\cos(a_k x)\sin(a_l y)+\\ \sum_{q=1}^{3}K_x^{coil}\cos[k(a_x x-\frac{2\pi}{3}(q-1))]\cdot\sin(la_y y)\end{array}\right] \quad (1)$$

$$B_y = \sum_{k=1,3...}^{\infty}\sum_{l=1,3...}^{\infty}\left[\begin{array}{l}K_{xy}^{pm}\sin(a_k x)\cos(a_l y)+\\ \sum_{q=1}^{3}K_y^{coil}\sin[k(a_x x-\frac{2\pi}{3}(q-1))]\cdot\cos(la_y y)\end{array}\right] \quad (2)$$

$$B_z = \sum_{k=1,3...}^{\infty}\sum_{l=1,3...}^{\infty}\left[\begin{array}{l}K_z^{pm}\sin(a_k x)\sin(a_l y)+\\ \sum_{q=1}^{3}K_z^{coil}\sin[k(a_x x-\frac{2\pi}{3}(q-1))]\cdot\sin(la_y y)\end{array}\right] \quad (3)$$

Where,

$$a=a_x=\frac{\pi}{\tau},\ a_y=\frac{\pi}{2\tau},\ a_k=ka,\ a_l=la$$

$$K_{xy}^{pm}=\frac{8aB_r}{\pi^2}\cdot\frac{k}{\lambda_{kl}D_{kl}}\left[C_{kl}J+\frac{1}{kl}\cos(a_l r_1)\cos(a_k r_1)\right]\cdot(\exp(\lambda_{kl}z)-\exp(2\lambda_{kl}l_{gm})\exp(-\lambda_{kl}z))$$

$$a_{kl}=\sqrt{k^2a_x^2+l^2a_y^2},\ r_1=\frac{\tau-p}{2}$$

$$\lambda_{kl}=\sqrt{a_k^2+a_l^2},\ l_{gm}=l_m+l_g$$

$$C_{kl}=\frac{a}{\lambda_{kl}}\left(\frac{1}{\tanh(\lambda_{kl}l_m)}-\frac{1}{\sinh(\lambda_{kl}l_m)}\right)$$

$$D_{kl}=\exp(\lambda_{kl}l_{gm})\sinh(\lambda_{kl}l_{gm})\frac{a}{\lambda_{kl}}\left(\frac{\mu_r}{\tanh(\lambda_{kl}l_m)}-\frac{1}{\sinh(\lambda_{kl}l_g)}\right)$$

$$J=\frac{1}{k}\cos(a_k r_1)\sin(a_l r_1)+\frac{1}{l}\cos(a_l r_1)\sin(a_k r_1)$$

$$M_{kl}=\frac{32N_tI}{k^2l^2\pi^2l_c}\cdot\frac{1}{a_xa_yw_c^2}\cdot\sin(ka_x\frac{w+w_c}{2})\sin(ka_x\frac{w_c}{2})\cdot\sin(la_y\frac{d+w_c}{2})\sin(la_y\frac{w_c}{2})$$

$$\beta^{\infty}=\frac{\mu_0M_{kl}\sinh(a_{kl}l_c)}{\cosh(a_{kl}l_c)\sinh(a_{kl}(l_c-l_{gm}))-\sinh(a_{kl}l_c)\cos(a_{kl}(l_c-l_{gm}))}$$

$$K_x^{coil}=-\frac{ka_x}{a_{kl}}\beta^{\infty}\cos(\frac{2\pi}{3}(q-1))\sinh(a_{kl}(l_{gm}-z))$$

$$K_y^{coil}=-\frac{ka_y}{a_{kl}}\beta^{\infty}\cos(\frac{2\pi}{3}(q-1))\sinh(a_{kl}(l_{gm}-z))$$

$$K_z^{pm}=\frac{8B_r}{\pi^2}\cdot\frac{k}{\lambda_{kl}D_{kl}}\left[C_{kl}J+\frac{1}{kl}\cos(a_l r_1)\cos(a_k r_1)\right]\cdot(\exp(\lambda_{kl}z)+\exp(2\lambda_{kl}l_{gm})\exp(-\lambda_{kl}z))$$

$$K_z^{coil}=-\cos(\frac{2\pi}{3}(q-1))\cdot\left[\beta^{\infty}\cosh(a_{kl}(l_{gm}-z))-\mu_0M_{kl}\right]$$

The other details can be seen in paper [4].

3. EXPERIMENTS AND ANALYSIS

A. Experiment equipments and methods

To verify the analysis propriety of analytical method, the experiments of flux density distribution of Halbach magnet array, back-EMF, and thrust of prototype machine of SPMPM have been done.

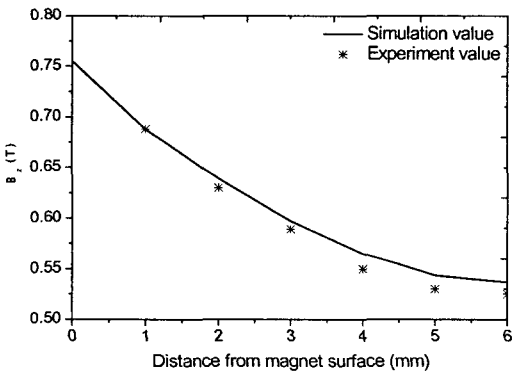

Fig. 3 The comparisons of flux density distribution

Fig. 3 shows the comparison of the flux density distribution between the simulation values and experiential results. The experiment values are measured by Gauss Meter and they agree with the simulation values well.

The back-EMF and thrust characteristics have been analyzed by the method in the paper [4]. The thrust is evaluated by means of Lorentz force. To verify the back-EMF and thrust characteristics, the experiments are implemented. Fig. 4 (a) shows the experimental equipments of Back-EMF and Fig. 4 (b) reveals the experiment equipments of thrust. In experiments, only the armature windings driving the mover in one direction are thought about.

In the experiment of back-EMF, the mover of prototype machine is connected with another linear motor at a speed of 1[m/sec], the induced voltage of armature windings is measured by Oscillo-Scope(model :LT364L).

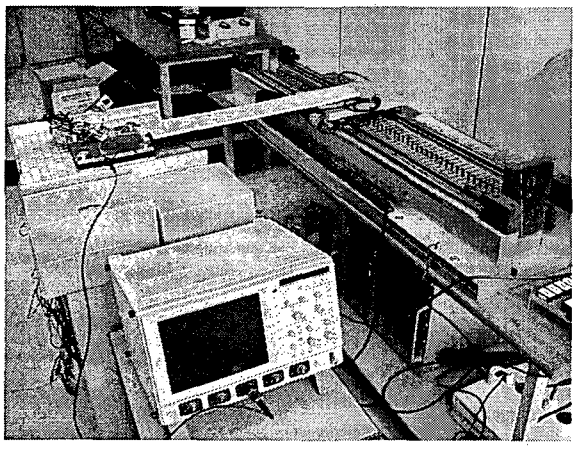

(a) Back-EMF experimental equipments

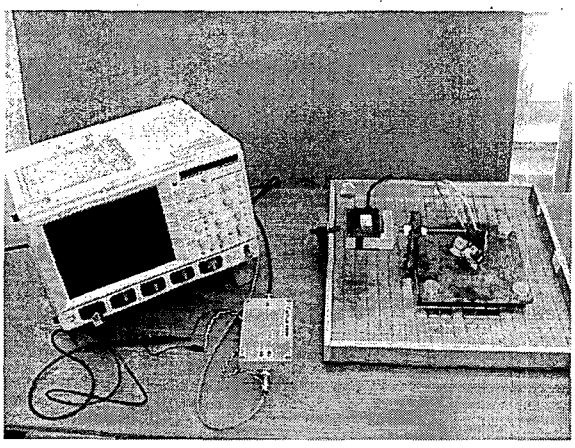

(b) Thrust experimental equipments

Fig. 4 Experimental equipments

The thrust is measured by load cell (model UU-K010 (cap. 10kgf), DACELL Co.). The three-phase current is supplied to the armature windings of prototype machine, output voltage of Load cell is measured by Oscillo-Scope(model LT364L). The magnitude of this voltage is very small and is amplified by the Amplifier (model STT-100, SCALE-TRON).

B. Experiment results and normal force analysis

Fig. 5 (a) shows the waveform of back-EMF. The simulation values and experiment values of back-EMF are shown in Fig. 5 (b), the peak experiment value of back-EMF is 11.80[V] and the maximum simulation value is 11.25[V], which is clearly described that the experiment results agree with the simulation values satisfactorily.

Fig. 6 reveals the comparison of thrust characteristic. In this case, the input current is 1[A], the thrust data calculated from the experimental values of back-EMF are close to simulation results well, but the values measured by Load cell are much smaller than both simulation values and the calculation ones from back-EMF. It is caused mainly by normal force acting as drag force in SPMPM.

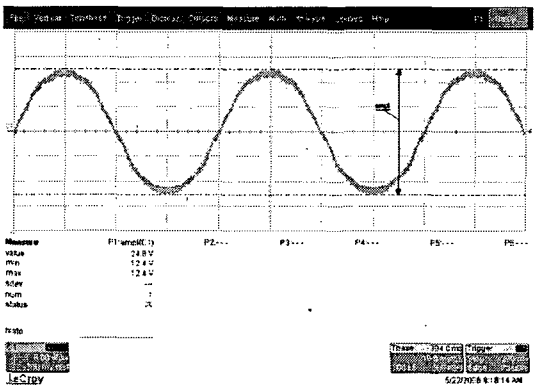

(a) Measured Back-EMF waveform of Oscillo-Scope

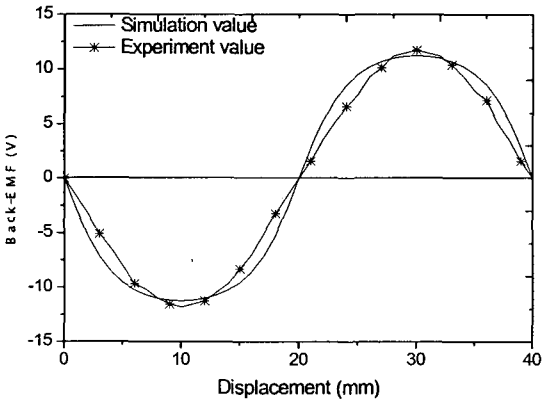

(b) Back-EMF comparison

Fig. 5 Back-EMF characteristic

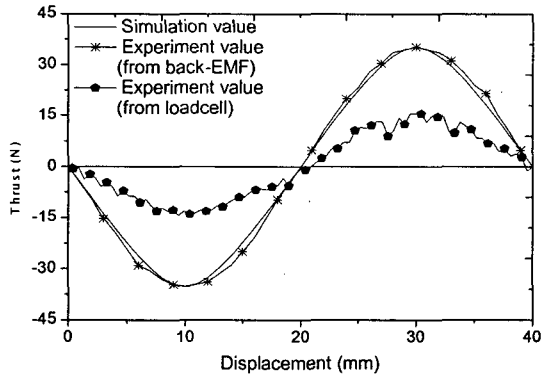

Fig. 6 Thrust characteristic

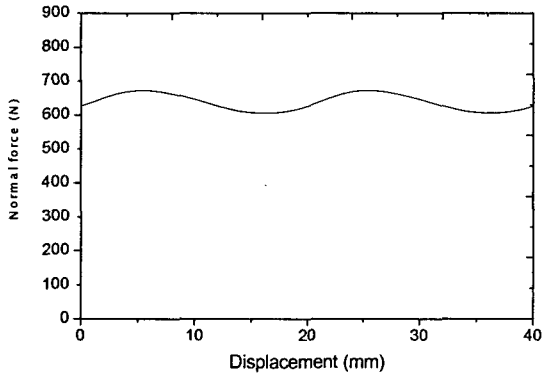

Fig. 7 The normal force characteristic

The normal force is analyzed by Maxwell stress tensor. Fig. 7 shows the normal force of the prototype machine, the peak value of the normal force is 672.83[N] when input current is 1[A] and it is about 19 times of the peak value of thrust which is 35.22[N], i.e. the maximum value of normal force is much larger than the peak value of thrust. Therefore, the measured values of thrust are much smaller than those of simulation because of the friction force generated by normal force.

C. The analysis of the effect caused by normal force

Fig. 8 reveals the experimental values and simulation ones of thrust according to the change of input current. To experimental values, in case of the input current of the armature windings is 2[A], the maximum experimental value of thrust is 32.27[N] which is 2.08 times of the peak experimental value of thrust, 15.51[N], when input current is 1[A]; if the input current is 3[A], the maximum experimental value of thrust is 80.67[N] and it is 5.20 times of the peak experimental value when input current is 1[A].

To simulation values, if the input current of armature windings is 2 [A], the peak value of thrust is 70.44[N] which is double of the peak simulation value of thrust, 35.22[N], when input current is 1[A]; and in case of the input current is 3[A], the maximum simulation value of thrust is 105.66[N] and is three times of the peak simulate value when input current is 1[A].

On the second thought, when the input current of armature windings is 1[A], the maximum experimental value of thrust is 44.04% of the peak simulation value; in case of the input current is 2[A], the ratio is 45.81%; and if the input current is 3[A], that ratio is 76.35%.

According to upper investigation, it can be concluded that the smaller the input current is, the stronger the undesired effect of the normal force is .

Furthermore, the undesired effect of normal force can be investigated by studying the behaviors of the friction force of SPMPM. According to mechanics theory, when the current is small, the thrust will not be big enough to overcome the static friction force which is caused by the normal force; as the current in coil increases, the thrust will be bigger than the maximum value of the static friction force, and the mover will move at once. While the mover moves, the sliding friction force is not bigger than the peak value of static friction force. Generally, the friction force change curve is shown as Fig. 9. F_s is the static friction force and $F_{sliding}$ is the sliding friction force. It indicates that when the input current is large enough to generate thrust which can overcome the peak value of static friction force and push mover into movement, the sliding friction force is not bigger than the maximum static friction force, i.e. the undesired effect of the normal force is reduced and the error between the experimental values of thrust and simulation values is decreased when input current increasing.

SPMPM is widely applied in automation field for it can move in 2-Dimensions. But like upper analysis, the normal force has an undesired effect on the thrust and the efficiency of the SPMPM will be low. Therefore, it is necessary to minimize the normal force.

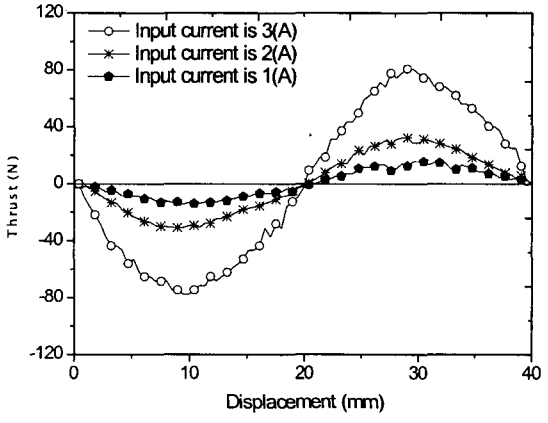

(a) Experimental values

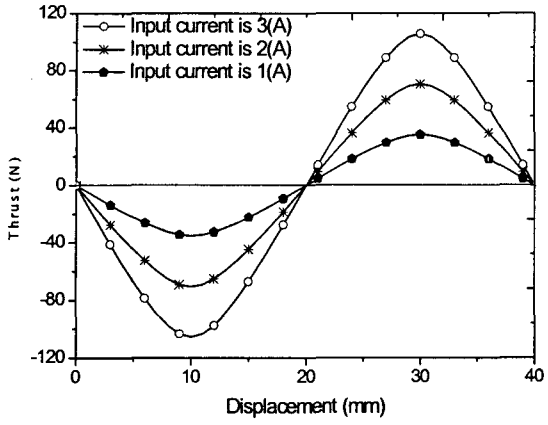

(b) Simulation values

Fig. 8 Thrust Characteristics

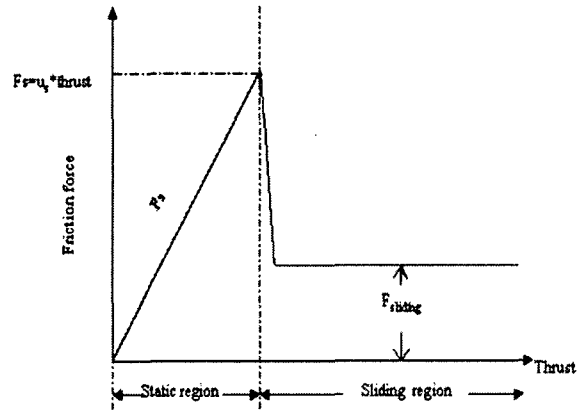

Fig. 9 The friction force change curve

4. NORMAL FORCE MINIMIZATION

A. Identification of the minimization problem

In the process of analysing the normal force, it is concluded that the normal force has a close relation with the dimensions of permanent magnet and armature windings. The key parameters of permanent magnet are the width p and the height l_m, the main dimensions of armature winding include its width w_c, its terminal length w, its effective length d, and its height l_c. In this minimization problem, above six parameters are selected as optimal variables and the detail is defined in Table 2. In this part, the input current is 1[A].

As a consequence, the problem is defined as:

Find a global best solution $\boldsymbol{x}=[x_1,x_2,\cdots,x_6]^T$

To minimize $f(\boldsymbol{x})=F_n(\boldsymbol{x})$ (4)

Where, $F_n(\boldsymbol{x})$ is normal force.

Some constraints are defined subsequently.

B. The constraints of minimization problem

There are some kinds of constraints of this minimization problem, regarding to search space, manufacture requirement and thrust. The search space boundary constraints are shown as Table 2. Other constraints are described as following

Table 2 Variables list

Variables	Boundary
x_1 : magnet width p	15 [mm]<= x_1 <=18[mm]
x_2 : magnet thickness l_m	5[mm]<= x_2 <=12[mm]
x_3 : coil terminal interval w	4[mm]<= x_3 <=9[mm]
x_4 : coil width w_c	4[mm]<= x_4 <=9[mm]
x_5 : coil effective length d	15[mm]<= x_5 <=20[mm]
x_6 : coil thickness l_c	4[mm]<= x_6 <=10[mm]

$$g_1(\boldsymbol{x}): F(\boldsymbol{x})-35\geq 0$$
$$g_2(\boldsymbol{x}): 1\leq 80/3-2x_4-1-x_3\leq 3$$

Where, $g_1(\boldsymbol{x})$ is the thrust constraints which is required larger than 35[N], $F(\boldsymbol{x})$ is the thrust function. $g_2(\boldsymbol{x})$ is the clear space between the align armature windings and is constrained in 1[mm] and 3[mm].

C. Minimization program

Genetic Algorithm(GA), as a powerful and broadly applicable stochastic search and optimization technique, is perhaps the most widely known type of Evolutionary Computation methods today for its advantages in large scale calculation. In the case of this minimization problem, there are over millions points in search space, so genetic algorithm with penalty function is used to solve the minimization problem. The fitness function is defined as following formula:

$$Fitness=f(\boldsymbol{x})+p(\boldsymbol{x}) \quad (5)$$

The penalty function,$p(\boldsymbol{x})$, is defined as following.

$$p(x)=\epsilon\left[w_1\times\sum_{i=1}^{c}\left\{\frac{g_i(x)}{g^*}\right\}+w_2\times\delta\sum_{i=1}^{c}\left\{\frac{\phi_i(x)}{\phi^*}\right\}\right] \quad (6)$$

Where, $g_i(x)$ and $\phi_i(x)$ are level of violation and amount of violation for the i-th constraint; w_1 and w_2 are weighting factors; g^* and ϕ^* are scaling factors; δ is penalty coefficient; ϵ is -1 for maximization and +1 for minimization. Assigned values for w_1, w_2, and δ are 0.2, 0.5, and 0.1 respectively.

In this study, we use the elementary operations of genetic algorithm, such as selection, crossover, and mutation. The population type is double vector and it can improve the accuracy of the solution. The elementary factors and parameters for genetic algorithm based on minimization, according to this case, are summarized in Table 3. The flow diagram of minimization problem is shown in Fig. 10.

The program of the process of generation iteration is made and the best values are the minimum value in generations.

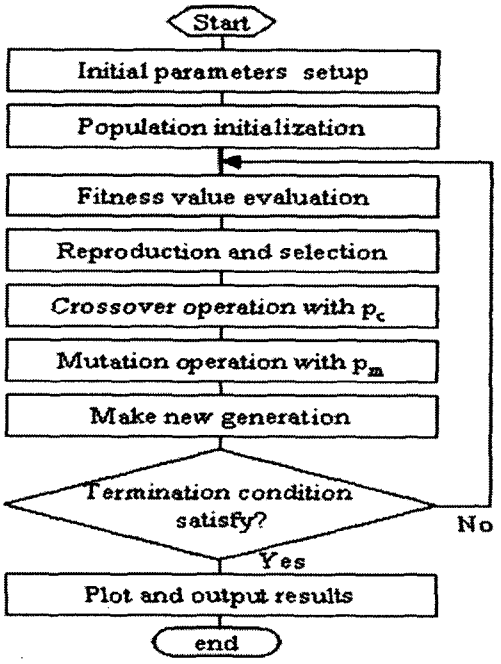

Fig. 10 The flow diagram of the genetic algorithm

D. Minimum results and investigation

The generation iteration process of genetic algorithm can be seen in Fig. 11, the fitness value is converged to 144.24 at the 920th generation, we had tried to continue optimization procedure over 1000 generations in order to check any further possible convergence point and the solution is same. The dimensions of the prototype

Table 3 Input parameters of genetic algorithm

Parameters	value
Number of variables	6
Population size	150
Population type	Double vector
Crossover fraction	0.8
Mutation fraction	0.05
Max number of generation	1000
Termination criteria	Max generation

machine are optimized and the results are shown in Table 4.

The contrast of characteristics between the original model and optimal model can be seen in Fig. 12. To the original model, the peak value of the normal force is decreased from 672.83N] to 144.24[N] remarkably shown in Fig. 12 (a), but the peak value of thrust is decreased from 35.22[N] to 35[N] shown in Fig. 12 (b).

According to the minimization results, there are two parameters, the thickness of permanent magnet and the thickness of armature winding, changed obviously. The reduction of the magnet thickness makes the decrease of the magnet flux density in air gap although the turns of armature windings are increased. The reason is that the magnet flux density generated by the permanent magnet is about 10 times of what generated by the current in armature windings. In the evaluation of thrust, it is analyzed by means of Lorentz force and the increased turns of armature windings give a big compensation to thrust. So the reduction of thrust is not so big. But, normal force, which is analyzed by Maxwell Tensor, the magnet flux density in air gap is a main contribution. Consequently, when the magnet flux density in air gap is reduced, the normal force is decreased obviously.

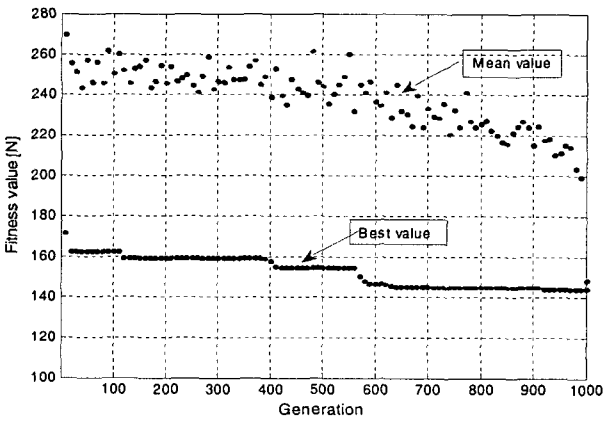

Fig. 11 The generation iteration process

Table 4 parameters and characteristics comparison

Symbols	Units	Original Model	Optimal Model
magnet width P	mm	18	18
magnet thickness l_m	mm	10	7
coil terminal interval w	mm	6.6	6.5
coil width w_c	mm	9	9
coil effictive length d	mm	20	19.4
coil thickness l_c	mm	6	10
Turns/phase		770	1284
Normal force	N	672.83	144.24
Thrust	N	35.22	35

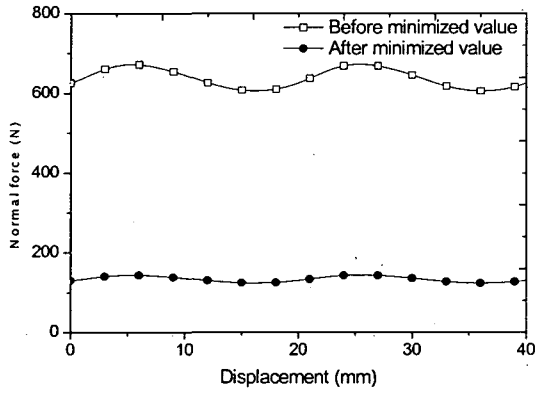

(a) The normal for0ce

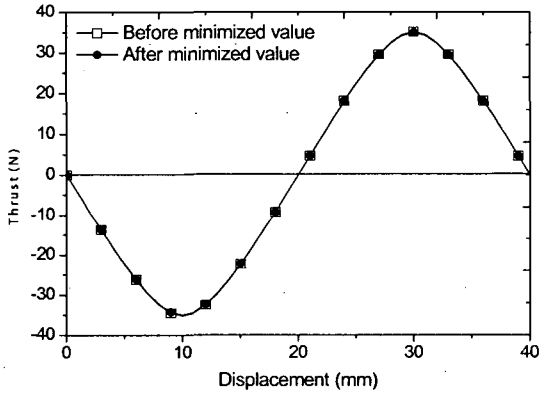

(b) The thrust

Fig. 12 The characteristics comparison

5. CONCLUSION

The characteristics of the SPMPM with Halbach magnet array are evaluated by the analytical method. By comparing the experiment values and simulation ones, the propriety of the analysis is verified.

By analyzing the error in experiment results of thrust, the undesired effect of normal force is analyzed in detail. Because of the undesired effect of the normal force, the efficiency of the SPMPM is low. So, in this paper, the genetic algorithm is applied to minimize normal force and normal force is remarkably decreased from 672.83[N] to 144.24[N].

감사의 글

본 연구는 2006년도 창원대학교 연구비 및 교육인적자원부·산업자원부·노동부의 출연금으로 수행한 산학협력중심대학육성사업의 연구결과입니다.

REFERENCES

[1] H. S. Cho and H. K. Jung, "Analysis and Design of synchronous permanent-magnet planar motors," IEEETrans. Energy Conversion, vol.17, pp.492-499, Dec.2002.

[2] H. S. Cho, C. H. Im, and H. K. Jung, "Magnetic field analysis of 2D permanent magnet array for planar motor," IEEE Trans. Magn., vol.37, pp.3762-3766, Sept. 2001.

[3] J. Y. Cao, Y. Zhu, J. S. Wang, W.S. Yin, and G. H. Duan, "A novel synchronous permanent magnet planar motor and its model for control applications," IEEE Trans. Magn., vol.41, pp.2156-2163,June.2005.

[4] Jianpei. Zhou, Rui. Huang, Donh-Yeup Lee, Gyu-Tak Kim, "Characteristics analysis of synchronous permanent magnet planar motor with Halbach array" The transactions on KIEE, vol .55B, no. 9, pp. 465 - 471, 2006.

저 자 소 개

김 덕 현 (金 德 顯)

1966년 7월 10일생. 1992년 한양대학교 전기공학과 졸업. 1996년 창원대학교 대학원 전기공학과 졸업(석사). 2002년 동 대학원 전기공학과 졸업(공박). 1991년~1996년 한화기계 자동화 사업부. 1997년~현재 건동대학교 기전공학부 조교수

Tel : 054-820-8133

E-mail : dh0710@kundong.ac.kr

김 규 탁 (金 奎 卓)

1961년 11월 12일생. 1982년 한양대학교 공대 전기공학과 졸업. 1984년 동대학원 전기공학과 졸업(석사). 1991년 동 대학원 전기공학과 졸업(공박).1996~2000년 일본 早稻田大 客員研究員. 현재 창원대학교 공대 전기공학과 교수.

Tel : 055-279-7515, Fax : 055-263-9956

E-mail : gtkim@sarim.changwon.ac.kr